Remote-sensing monitoring of desertification, phenology, and droughts

Arnon Karnieli and Giorgio Dall'Olmo
J. Blaustein Institute for Desert Research, Ben-Gurion University of the Negev, Sede-Boker Campus, Israel

Keywords *Environment, Geographical information systems, Israel, Egypt*

Abstract *Year-to-year fluctuations of rainfall in the northern Negev desert provide an opportunity to characterize and assess the temporal dynamics of desertification, phenology, and drought processes. Such information was retrieved and analyzed by combined use of satellite imageries in the reflectivity and thermal spectral bands. Data covering four years of coarse spatial resolution and images from a high revisit time satellite, namely the NOAA-14, were used. The images were processed to produce the normalized difference vegetation index (NDVI) and the land surface temperature (LST). These measures were applied to the sand field in the northwestern Negev (Israel), which is almost totally covered by biological soil crusts, and to an adjacent region in Sinai (Egypt), consisting mainly of bare dune sands. Various manipulations of the data were applied. Time series presentation of the NDVI and LST reveals that the NDVI values correspond to the reaction of the vegetation to rainfall and that LST values represent seasonal climatic fluctuation. Scatterplot analysis of LST vs NDVI demonstrates the following: the two different biomes (Sinai and the Negev) exhibit different yearly variation of the phenological patterns (two seasons in Sinai moving along the LST axis, and three seasons in the Negev, where the NDVI axis represents the growing season); the Sinai has an ecosystem similar to that found in the Sahara, while the Negev, only a few kilometers away, has an ecosystem similar to the one found in the Sahel; and drought indicators were derived by using several geometrical expressions based on the two extreme points of the LST-NDVI scatterplot. The later analysis led to a discrimination function that aims to distinguish between the drought years and the wet years in both biomes. Results from the current study show that a great deal of information on dryland ecosystems can be derived from four, out of five, NOAA/AVHRR spectral bands. The NDVI is derived from the red and the near-infrared bands and the LST from the two thermal bands. Combined use of these two products provides more information than any product alone.*

Introduction

The severe recurrence of droughts in the Sahel and other regions, as well as an apparent accelerated southward advance of the Sahara Desert, led to extensive international discussions and to the establishment of the United Nations Conference on Desertification (UNCOD). At this meeting, desertification was defined as "land degradation in arid, semi-arid, and dry sub-humid areas resulting mainly from adverse human impact" (UNEP, 1992).

The term "phenology" is usually defined as "the study of the timing of recurring biological phases, the cause of their timing with regard to biotic and

Management of Environmental Quality: An International Journal
Vol. 14 No. 1, 2003
pp. 22-38

1477-7835
DOI 10.1108/14777830310460360

The authors would like to thank Mr Qin Zhihao for processing the thermal data.

abiotic forces, and the interaction among phases of the same or different species" (Lieth, 1974). The current study deals with natural vegetation phenology, rather than that of agriculture.

Drought can be defined as a period of abnormally dry weather, which persists long enough to produce a serious ecological, agricultural, or hydrological imbalance (e.g. crop damage, water shortage, etc.). The severity of the drought depends upon the degree of moisture deficiency, the duration, and the size of the affected area. In this context, meteorological drought refers to lower than average precipitation for some time period (Wilhite and Glantz, 1985).

These three basic dryland processes, namely desertification, phenology, and drought, are strongly linked. Drought is part of the cause of desertification and certainly makes the situation worse. Mainguet (1994) states that desertification is "revealed by drought". The phenology of natural plants is changed by either desertification or drought processes. It is expressed, for example, by changes between grasses and shrubs, C3 and C4 species, or palatable to unpalatable species. The objective of the current paper is to characterize and assess the temporal dynamics of these three processes, by jointly analyzing reflective and thermal data acquired by satellite remote sensing means.

The advanced very high resolution radiometer (AVHRR), operated by the National Oceanic Atmospheric Administration (NOAA), with 1km spatial resolution and high temporal resolution of about one day, plays a significant role in monitoring regional and global processes. The most important AVHRR-derived products for ecological applications are the normalized difference vegetation index (NDVI) and the land surface temperature (LST).

The NDVI was formulated by Rouse *et al.* (1974) as:

$$\mathrm{NDVI} = (\rho_{\mathrm{NIR}} - \rho_{\mathrm{R}})/(\rho_{\mathrm{NIR}} + \rho_{\mathrm{R}}), \tag{1}$$

where ρ is the reflectance in the red (R) and near-infrared (NIR) bands of the NOAA/AVHRR sensor. This index, as well as several other modifications of it that are less common, are based on the difference between the maximum absorption of radiation in the red (due to the chlorophyll pigment), and the maximum reflection of radiation in the NIR (due to the leaf cellular structure and the fact that soil spectra, lacking these mechanisms, typically do not show such a dramatic spectral difference). The NDVI has been proven to be well correlated with various vegetation parameters, such as green biomass (Tucker, 1979), chlorophyll concentration (Buschmann and Nagel, 1993), leaf area index (Asrar *et al.*, 1984), foliar loss and damage (Vogelmann, 1990), photosynthetic activity (Sellers, 1985), carbon fluxes (Tucker *et al.*, 1986), phenology (Justice *et al.*, 1985), and others. Also, they have been found to be useful for a variety of image analyses like crop classification (Ehrlich and Lambin, 1996), green coverage (Elvidge and Chen, 1995), and change detection (Lambin and Strahler, 1994).

The retrieval of LST from NOAA-AVHRR data is achieved mainly through the application of so-called split window (Price, 1984). Several split window algorithms have been developed on the basis of various considerations of the effects of the atmosphere and the emitting surface, derived from the equation of thermal radiation and its transfer through the atmosphere. However, the effect of the atmosphere is so complex, that any treatment is difficult. Therefore, various simplifications have been assumed for the derivation that has led to the establishment of different forms of split window algorithm (Qin and Karnieli, 1999). Thus, if T4 and T5 are the brightness temperatures in bands 4 and 5 of AVHRR data, respectively, which are given by inverting Planck's equation for the radiation received by the sensor, the general form of split window algorithm can be expressed as:

$$LST = T4 + A(T4 - T5) + B, \quad (2)$$

where A and B are the coefficients affected by the atmospheric transmittance and surface emissivity in spectral bands 4 and 5 of AVHRR data. All temperatures in the equation are in degrees of Kelvin. The theoretical accuracy of the LST can reach ± 1.6°C.

Study area

Perhaps the most spectacular phenomenon connected with desertification vs rehabilitation can be observed across the Israel-Egypt political border (Figure 1). Although the sand field of the Negev desert (Israel) represents the eastern extension of the Sinai (Egypt) fields from the geomorphological and

Note: The high contrast across the borderline is due to almost complete cover of soil biological crusts in the Negev and absence of them in Sinai

Figure 1.
Location map based on NOAA-AVHRR image showing the study polygons on both sides of the border between Israel and Egypt

lithological points of view, the area is artificially divided by the political borderline. The borderline is characterized by a sharp contrast; higher reflectance values (brighter) on the Egyptian side and lower reflectance values (darker) on the Israeli side. This contrast has long drawn the attention of many scientists. The traditional and popular explanation asserts that the contrast is mainly due to severe anthropogenic impact of the Sinai Bedouin, especially overgrazing by their black goat and sheep herds, as well as gathering of plants for firewood. The Israeli side of the border has been subject to a conservation of nature policy since the 1950s and especially, under an advanced rehabilitation process since 1982. This interpretation was pioneered by Otterman (1974) and summarized in Otterman (1996). Classification based on satellite and aerial photographs revealed that the Sinai is dominated by bare sands (83.5 percent) while in the Negev, the sands are overlaid by soil biological crusts (71 percent) (Table I). Consequently, Sinai is characterized by shifting sand dunes while these dunes have been stabilized in the Negev. As a result, a new theory, recently proposed by Karnieli and Tsoar (1995) and Tsoar and Karnieli (1996), suggests that the contrast is not a direct result of severe overgrazing of higher vegetation but is caused by an almost complete cover of biological soil crusts on the Israeli side, while human and animal activities have prevented the establishment and accumulation of such crusts, as well as trampling and breaking up any existing crusts on the Egyptian side.

Mean annual rainfall in the study area is 90mm. The current project lasted four years from October 1995 to September 1999. Two of these years were relatively dry (drought) years – 1995/1996 and 1998/1999 – with 32.3 and 31.2mm rainfall, respectively. The other two years were relatively wet – 1996/1997 and 1997/1998 – with 79.3 and 83.6mm rainfall, respectively.

Methodology

The NOAA-AVHRR data were acquired in high-resolution picture transmission (HPRT) format (-1×1km) by the ground receiving station located at the Sede Boker Campus (Negev, Israel). NOAA-14 images were obtained for four years from October 1995 to September 1999. The geometrical distortion introduced by the large scan angle was reduced by limiting the use of the images to those with a satellite zenith angle of 30° and by using only cloud-free images.

	Negev (%)	Sinai (%)
Bare sands/playas	11	83.5
Biological soil crusts	71	12
Perennials	18	4.5

Note: Based on Qin (2001)

Table I. Percentage ground cover of different ground features in the Negev (Israel) and Sinai (Egypt)

Three types of pre-processing were used in the study:

(1) radiometric;

(2) atmospheric; and

(3) geometric corrections.

The processing of the data in the visible and NIR bands was based on post-launch calibration coefficients suggested by NOAA/NESDIS (Rao and Chen, 1998). Atmospheric correction of the top-of-atmosphere reflectances was carried out using the 6S code, including correction for molecular scattering, while geometry of the sensor and the sun was also applied (Vermote *et al.*, 1997). This program also requires estimates of the water vapor, aerosol, and ozone contents in the atmosphere. The total precipitable water and aerosol optical thickness of the atmosphere were obtained from an automatic tracking sun photometer (CIMEL), installed at Sede Boker, about 50km away from the study area (Holben *et al.*, 2001). Ozone content in the atmosphere was based on climatology derived from the total ozone mapping spectrometer (TOMS) onboard the Nimbus-7 spacecraft between 1987 and 1993. The images were geometrically corrected to a master image, using ground control points and applying a nonlinear second order transformation. The accuracy of the correction lies at the subpixel level. One subset of 150 pixels on each side of the border (about $15 \times 10 \text{km}^2$) was extracted, assuming homogeneous areas from each image (Figure 1). The NDVI values were calculated from the surface reflectance values of the red and NIR bands of the AVHRR images.

Radiometric correction of the two NOAA AVHRR thermal bands, 4 and 5, was performed following Brown *et al.* (1995) and Weinreb *et al.* (1990). Geometric correction and subset extraction were applied to the red and NIR bands. These operations were necessary at this early step of the processing in order to later apply the local characteristics of the split window algorithm (Qin *et al.*, 2001), used to correct the atmospheric influence on the thermal infrared bands. The algorithm used has a modified form of equation (2) that requires total precipitable water and surface emissivity to compute the constants. The first constant was obtained from the CIMEL data, relative to the image date of acquisition; the second was estimated by laboratory analysis of soil samples taken in the study area (Qin, 2001). Based on this work, the emissivity value of bare sand dunes (average value of 0.95) was assigned to the Sinai's polygon, while the emissivity value of the biological soil crusts (average value of 0.97) for that of the Negev. The maximum value composite (MVC) method (Holben, 1986) was applied to the NDVI and LST values for a one-month composition period.

Analysis and results

Temporal dynamics of NDVI and LST

The temporal variations of the NDVI and the LST along the four hydrological years of the project are presented in Figure 2. Figure 2A shows that the Negev

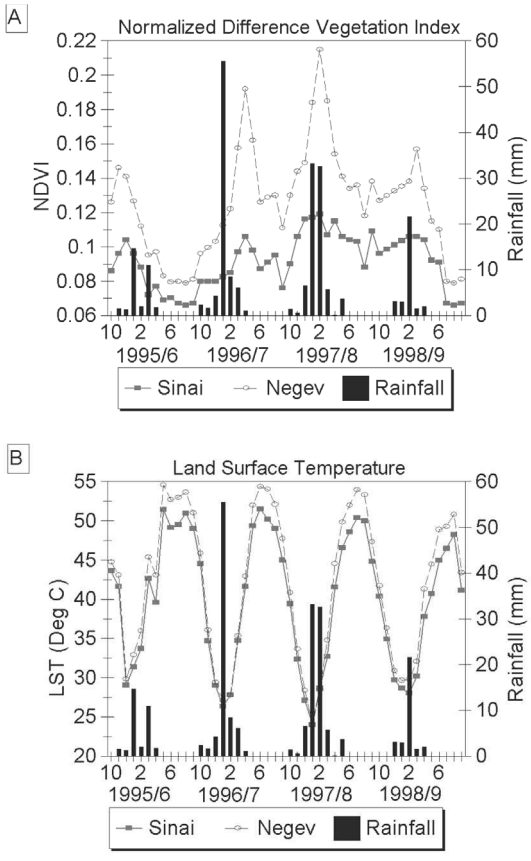

Note: The NDVI values correspond to the reaction of the vegetation to rainfall and that LST values represent seasonal climatic fluctuation

Figure 2.
Temporal variations of NDVI (A) and LST (B) in Sinai and the Negev along the four hydrological years of research

ecosystem, under an advanced rehabilitation process since 1982, shows higher values of vegetation index (mean NDVI for the whole data set= 0.124 ± 0.039) and high reactivity to rainfall (from 0.116 ± 0.033 during the dry period to 0.143 ± 0.045 in the wet period), especially during wet years (1996/1997 and 1997/1998). In contrast, the Sinai area, under desertified conditions, presents a very low reaction to rainfall (from 0.086 ± 0.014 during the dry period to 0.096 ± 0.015 in the wet period), maintaining approximately constant NDVI values (mean NDVI for the whole data set = 0.089 ± 0.015). A slight increase in the vegetation index is visible only during the wet years. The differences between the mean NDVI values of Negev and Sinai can be as high as 0.1, following the rainy season of a wet year. Since it is well known that higher NDVI values are caused by a dark soil background (Huete, 1988), NDVI

differences during the dry periods seem to be related to the brightness difference between the two sides of the border, due to the presence of the dark biological soil crusts and, to a lesser extent, the higher vegetation on the Israeli side (Karnieli and Tsoar, 1995).

Figure 2B demonstrates the monthly MVC values of the computed LST in the sampling polygons on both sides of the border. No clear differences in phase are evident. On the contrary, the cyclical temperature trends are similar in the Negev and in Sinai and follow the climatic variations throughout the four years. During the relatively wet winters, evaporation determines large losses of energy from the wet soil surface; low sun irradiance also contributes less significantly than in summer to the soil heat balance. Thus, the minimum LST values are always found in the rainy period during the winter, and can be as low as 20°C. In these seasons, the difference in the amplitude between the polygons is almost negligible. The maximum temperatures are found at the height of summer and can reach values of 58°C. The temperature differences between the two sides of the border can be as high as 7°C.

The explanations for the amplitude differences evident in the dry period are addressed in Qin *et al.* (2001). Since the sand dunes on the Israeli side are almost completely covered by dark biological soil crusts, they absorb more incident radiation and emit stronger thermal radiation than the bare sand on the Egyptian side. Moreover, although more higher and lower vegetation is present on the Israeli side, these desert plants, due to their scarcity and dormancy in the hot, dry summer, contribute almost nothing to the regional evapotranspiration that cools the surface. Thus, in the dry season, the Israeli side presents higher values of surface temperatures than in the Sinai.

Desertification assessment

The combination of reflective and thermal data for determining soil water status or surface water availability has been reported in numerous studies (Goward and Hope, 1989; Nemani *et al.*, 1993; Lambin and Ehrlich, 1996; 1997). This type of analysis has usually been undertaken by plotting LST against NDVI values (Figure 3A). Such a method is used in the current research in order to characterize the desertification processes in the study area. A scatterplot of multi-year NDVI vs LST values was created (Figure 3B). Applying a K-mean analysis of two clusters for the data, it was shown that the combined values of the Negev are significantly different from those of Sinai. Comparing the location of the clusters to the African continental scheme of Lambin and Ehrlich (1996), the current scatterplot demonstrates that the Sinai desertified ecosystem overlaps the area covered by the Sahara biome, while the Negev recovered side of the border, although located only a few kilometers away, exhibits characteristics similar to those of the Sahel biome (although it fits even better to that in the Southern African hemisphere, discussed in the same paper).

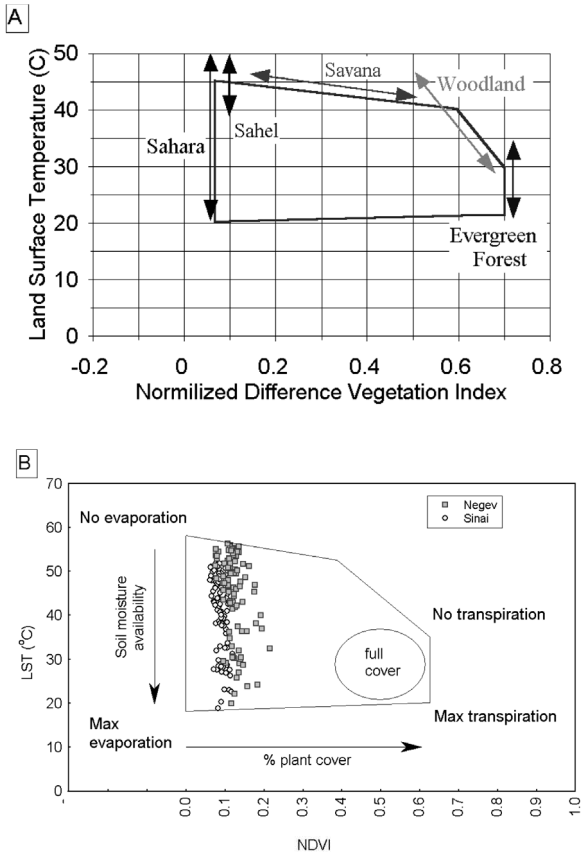

Source: After Lambin and Ehrlich (1996)

Note: The Sinai has an ecosystem similar to that found in the Sahara, while the Negev, only a few kilometers away, has an ecosystem similar to the one found in the Sahel

Figure 3.
(A) Scatter diagram for schematic discriminating of different biomes in Africa as proposed by Lambin and Ehrlich (1996). (B) Data obtained for this study

Phenology

Results of the K-mean analysis reveal that 5 clusters characterize the study area (Figure 4). Statistics for each cluster are described in Table II. The Sinai area, under a desertification process, is characterized by just two clusters (1 and 2) corresponding to the dry and wet seasons respectively, and defined by the fluctuations of land surface temperatures throughout the year. In this area, the biological activity is almost non-existent, therefore only the physical meteorological factors are responsible for the movement inside the LST-NDVI space. On the other hand, the recovered ecosystem of the Negev shows relatively intense biological activity and is characterized by movements over

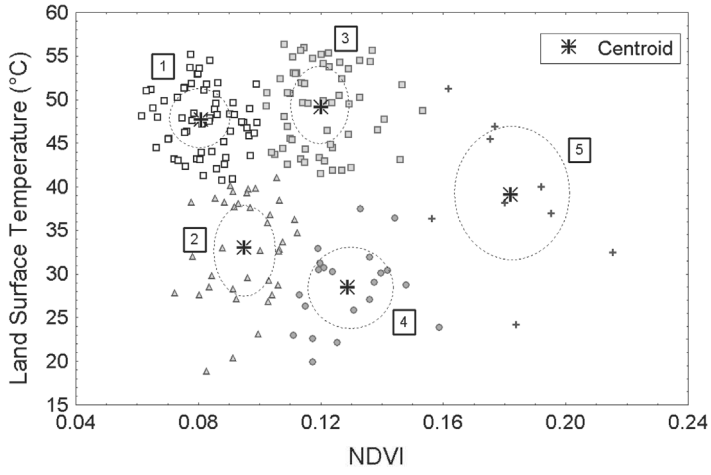

Note: The numbers in the square boxes refer to the cluster numbers mentioned in the text and in Table II. The dashed lines represent one standard deviation from each centroid (after Dall'Olmo and Karnieli, 2002). The two different biomes (Sinai and the Negev) exhibit different yearly variation of the phenological patterns: two seasons in Sinai (clusters 1 and 2) moving along the LST axis; and three seasons in the Negev (clusters 3, 4 and 5) where the NDVI axis represents the growing season

Figure 4.
Groups obtained from the cluster analysis of NDVI and LST data

Cluster	Season	No. of Negev pixels	No. of Sinai pixels	Mean NDVI (SD)	Mean LST (SD)
1	Dry	14	48	0.082 (0.010)	47.7 (3.6)
2	Rainy	4	33	0.095 (0.010)	33.0 (5.8)
3	Dry	51	7	0.120 (0.012)	49.2 (4.6)
4	Rainy	16	5	0.123 (0.013)	28.5 (4.6)
5	Growing	9	0	0.182 (0.018)	39.1 (8.1)

Note: Based on Dall'Olmo and Karnieli (2002)

Table II.
Description of the clusters obtained from the NDVI and LST data analysis

three clusters of the LST-NDVI space. In the Negev ecosystem, as in the Sinai, both dry and rainy seasons are evident (clusters 3 and 4) while the third cluster (number 5) represents the growing season, which is evident only on the Israeli side of the border and which includes the highest values of NDVI. Only a few points are presented inside cluster number 5, because it corresponds to the very short period of the year in which the desert reaches its maximum greenness due to the blooming of the annuals.

It is interesting to note that several points belonging to the Negev are located inside cluster 1, which represents the Sinai. The explanation for this fact can be found in Holling (1973). Natural arid land systems show a resilient character rather than a resistant one: their stability is not defined by a unique equilibrium

state, but according to fluctuations of environmental parameters. Beyond certain limits, they can be associated with multiple-equilibrium states of a domain, inside which the ecosystem does not change its structure. This is the result of adaptation to the harsh, extremely variable desert environment. The overlapping points of cluster 1 are relative to the very dry years (1995/1996 and 1998/1999). In periods extremely lacking in water, the recovered ecosystem is able to reduce its activity to the minimum needed for surviving in the area of the LST-NDVI space typical of desertified ecosystems. However, as soon as the precious resource of water is available again, it can immediately react and produce relatively high values of NDVI. On the other hand, the disturbed ecosystem (Sinai) shows the result of a man-made perturbation that has changed its structure: in wet years only an extremely limited response to rainfall is detected.

The multi-year average of the combined NDVI and LST values are presented in Figure 5 in terms of month-by-month trajectories. Phenology starts in October and ends in September of the following year. It is shown that the desertified Sinai ecosystem exhibits the highest variability mostly along the LST axis and is almost unaffected by the NDVI, except for a slight deviation from the straight line between April and July, most likely due to some greenness of perennials. On the other hand, the recovered Negev side of the border exhibits variability on both LST and NDVI axes. Here, the NDVI axis is dominant especially during the wet months (January-July) due to the greening of biological soil crusts, annuals, and perennials. During the summer months, the trajectory moves only along the LST axis.

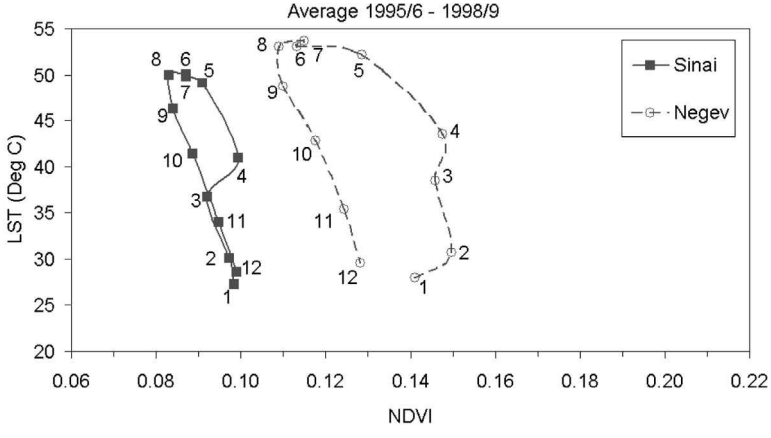

Note: The desertified Sinai ecosystem exhibits the highest variability mostly along the LST axis and is almost unaffected by the NDVI. On the other hand, the recovered Negev side of the border exhibits variability on both LST and NDVI axes

Figure 5.
Multi-year average of the combined NDVI and LST values in terms of month-by-month trajectories

Drought assessment

Figure 6 exhibits the breakdown of Figure 5 into the four hydrological years under investigation, to demonstrate the annual dynamics. In the Sinai, little difference can be seen between the wet and the dry years, with the same general trajectory shape – long, narrow, and with a vertical pattern along the LST axis. In the Negev, however, there is a considerable difference between the wet and dry years. During the wet years (1996/1997 and 1997/1998) the shape of the graphs is stretched towards the high NDVI values and the phenological cycle is much more pronounced, whereas during droughts (1995/1996 and 1998/1999) the NDVI component is much less remarkable and the phenological cycle shrinks significantly.

Figure 7 shows, for each of the hydrological years and for the Negev and Sinai ecosystems separately, the lines connected between two points defined as:

(1) the maximum LST − minimum NDVI; and

(2) minimum LST − maximum LST.

It may be seen that the Sinai lines are very similar in terms of position and length; however, two groups can be distinguished between the Negev lines. The lines of the wet years are longer and with gentler slopes, whereas the dry years lines are shorter and steeper. These characteristics can be quantified by three geometrical expressions as schematically illustrated in Figure 8:

$$\text{Angle} = \arctan(\Delta\text{LST}/\Delta\text{NDVI}), \tag{3}$$

$$\text{Area} = \Delta\text{NDVI} * 0.5\Delta\text{LST}, \tag{4}$$

$$\text{Length} = [(\Delta\text{LST})^2 + (\Delta\text{NDVI})^2]^{0.5}. \tag{5}$$

These three expressions can be used as indicators for quantifying drought years. Their calculated values are presented in Table III. Evaluation of the three indicators was performed by applying the following discrimination function (DF) for each year (i) and each region (j):

$$DF_{ij} = (X_{ij} - X_{meanj})/(X_{maxj} - X_{minj}),$$

where X_{ij} is the calculated value for each indicator, either in Sinai or in the Negev, in any particular year. X_{avg}, X_{max}, and X_{min}, are the yearly average, maximum and minimum values for each region, respectively. The objective of this function is to discriminate the drought years from the wet years on both sides of the border.

Results of the discrimination function for each of the drought indicators are presented in Figure 9. It can be noticed that for the Negev, each of the indicators successfully separates the two drought years from the wet years, since the DF_{ij} receives either positive or negative values. However, for Sinai, only the "length"

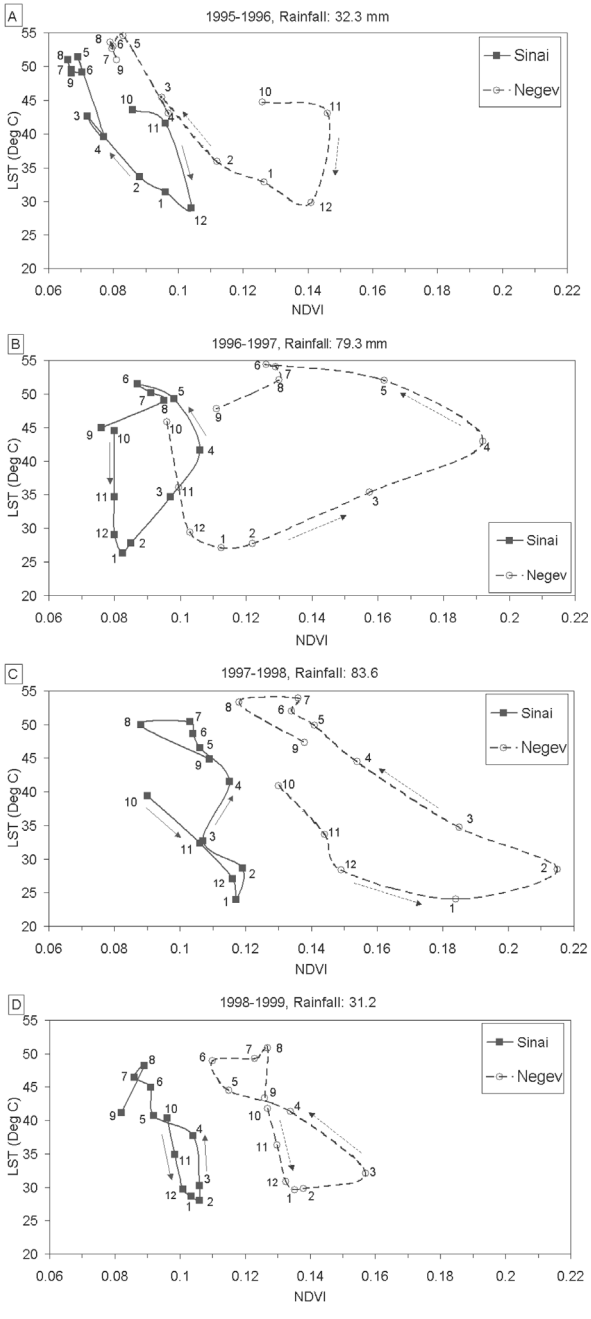

Note: Note differences between the drought years (1995/1996 and 1998/1989) and the normal years (1996/1997 and 1997/1998)

Figure 6.
Trajectories of conmined NDVI and LST values for each of the four hydrological years (October (10) → September (9))

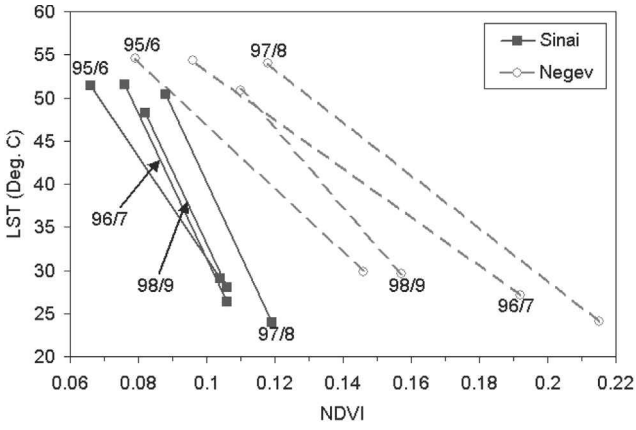

Note: Note differences in slope and length of the lines between the two biomes and among years

Figure 7.
Lines connected between maximum LST/minimum NDVI and minimum LST/maximum NDVI for the Sinai and the Negev

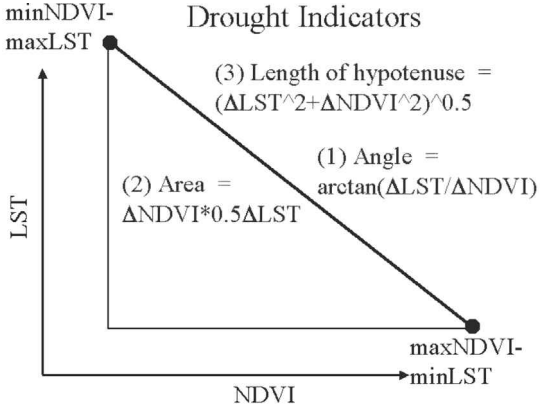

Figure 8.
Schematic illustration of three geometrical expressions for indicating droughts

	Year	Sinai	Negev
Angle	1995/1996	80.36	74.85
	1996/1997	83.20	70.63
	1997/1998	83.31	72.06
	1998/1999	83.23	77.78
Area	1995/1996	0.43	0.83
	1996/1997	0.38	1.31
	1997/1998	0.41	1.45
	1998/1999	0.24	0.50
Length	1995/1996	22.38	24.75
	1996/1997	25.16	27.31
	1997/1998	26.42	29.95
	1998/1999	20.22	21.17

Table III.
Calculated values for the three drought indicators

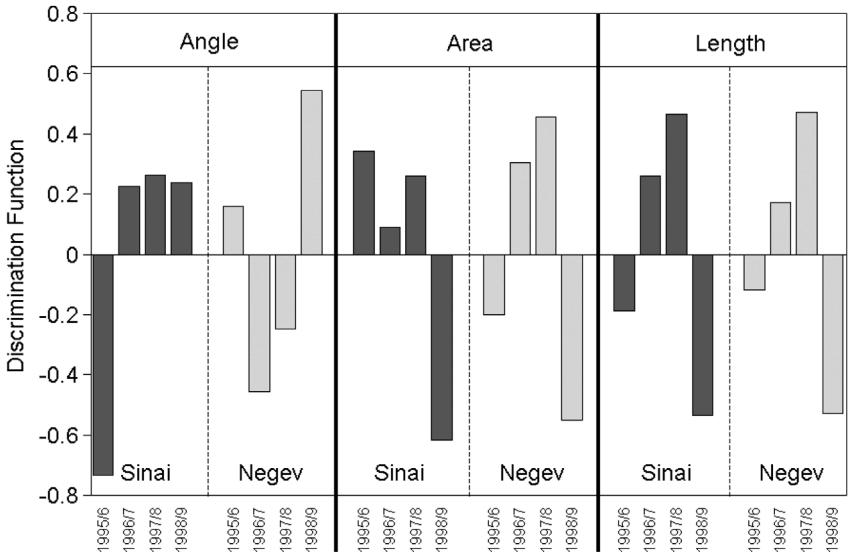

Figure 9.
Results of the discrimination function procedure for each drought indicator

indicator is able to show this phenomenon. The other two indicators – slope and angle – produce mixed results. Consequently, the "length" indicator will be used for further analysis.

Using the "length" indicator, Figure 10 presents the DF_j values as a function of the yearly rainfall of each year. Despite the fact that only eight points are involved in the regression analysis, a clear trend is exhibited between the drought-year cluster (negative values) and the wet-year cluster (positive

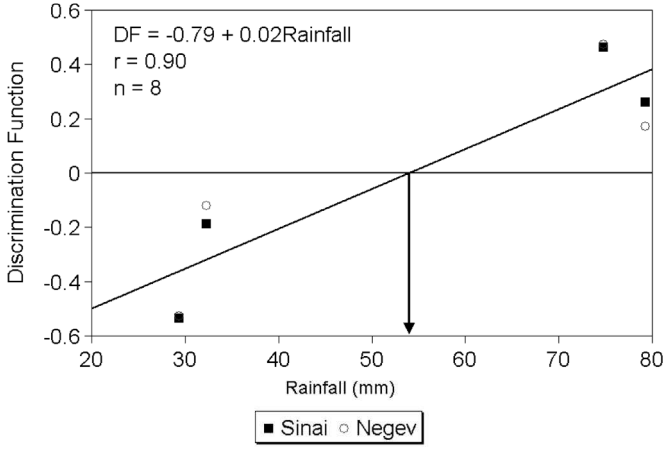

Note: The crossing point between the regression line and the DF = 0 line can be used to quantify the threshold between wet and drought years in terms of rainfall amount

Figure 10.
Discrimination function values vs the yearly rainfall amounts of each year

values). The crossing point between the regression line and the DF= 0 line can be used to quantify the threshold between wet and drought years in terms of rainfall amount (54mm in the current example).

Summary and conclusions

Results from the current study show that desertification, phenology, and droughts processes can be detected and characterized by using four out of five NOAA/AVHRR spectral bands. The NDVI is derived from the red and the NIR bands and the LST from the two thermal bands. Combined use of these two products provides more information than any product alone.

Time series presentation of NDVI and LST reveals that the NDVI values correspond to the reaction of the vegetation to rainfall and that LST values represent seasonal climatic fluctuation. Scatterplot analysis of LST vs NDVI demonstrates the following:

- The two different biomes (Sinai and the Negev) exhibit different yearly variations of the phenological patterns: two seasons in Sinai moving along the LST axis, and three seasons in the Negev, where the NDVI axis represents the growing season.
- The Sinai has an ecosystem similar to that found in the Sahara while the Negev, only a few kilometers away, has an ecosystem similar to that of the Sahel.
- Drought indicators were derived in terms of three geometrical expressions based on the two extreme points of the NDVI-LST scatterplots. Evaluation of the suggested indicator shows only one that can successfully separate between the drought and the wet years. It is concluded that the AVHRR imagery can provide valuable information for drought monitoring and characterization.

References

Asrar, G., Fuchs, M., Kanemasu, E.T. and Hatfield, J.L. (1984), "Estimating absorbed photosynthetic radiation and leaf area index from spectral reflectance of wheat", *Agronomy J.*, Vol. 76, pp. 300-6.

Brown, O.B., Brown, J.W. and Evans, R.H (1985), "Calibration of advanced very-high resolution radiometer infrared observations", *J. Geophys. Res.*, Vol. 90 C6, pp. 11667-77.

Buschmann, C. and Nagel, E. (1993), "In vivo spectroscopy and internal optics of leaves as basis for remote-sensing of vegetation", *Int. J. Remote Sens.*, Vol. 14, pp. 711-22.

Dall'Olmo, G. and Karnieli, A. (2002), "Following phenological cycles of desert ecosystems using NDVI and LST data derived from the advanced very high resolution radiometer", *Int. J. Remote Sens.*, Vol. 23.

Ehrlich, D. and Lambin, E.F. (1996), "Broad scale land-cover classification and interannual climatic variability", *Int. J. Remote Sens.*, Vol. 17, pp. 845-62.

Elvidge, C.D. and Chen, Z.K. (1995), "Comparison of broad-band and narrow-band red and near-infrared vegetation indexes", *Remote Sens. Environ.*, Vol. 54, pp. 38-48.

Goward, S.N. and Hope, A.S. (1989), "Evaporation from combined reflected solar and emitted terrestrial radiation: preliminary FIFE results from AVHRR data", *Adv. in Space Res.*, Vol. 9, pp. 239-49.

Holben, B.N. (1986), "Characteristics of maximum-value composite images from temporal AVHHR data", *Int. J. Remote Sens.*, Vol. 7, pp. 1417-34.

Holben, B.N., Tanre, D., Smirnov, A., Eck, T.F., Slutsker, I., Abuhassan, N., Newcomb, W.W., Schafer, J.S., Chatenet, B., Lavenu, F., Kaufman, Y.J., Castle, J.V., Setzer, A., Markham, B., Clark, D., Frouin, R., Halthore, R., Karneli, A., O'Neill, N.T., Pietras, C., Pinker, R.T., Voss, K. and Zibordi, G. (2001), "An emerging ground-based aerosol climatology: aerosol optical depth from AERONET", *J. Geophys. Res.-Atmos.*, Vol. 106 D11, pp. 12067-97.

Holling, C.S. (1973), "Resilience and stability of ecological systems", *Ann. Rev. of Ecology and Systematics*, Vol. 4, pp. 1-23.

Huete, A. (1988), "A soil-adjusted vegetation index (SAVI)", *Remote Sens. Environ.*, Vol. 25, pp. 295-309.

Justice, C.O., Townshend, J.R.G., Holben, B.N. and Tucker, C.J. (1985), "Analysis of the phenology of global vegetation using meteorological satellite data", *Int. J. Remote Sens.*, Vol. 6, pp. 1271-318.

Karnieli, A. and Tsoar, H. (1995), "Spectral reflectance of biogenic crust developed on desert dune sand along the Israel-Egypt border", *Int. J. Remote Sens.*, Vol. 16, pp. 369-74.

Lambin, E.F. and Ehrlich, D. (1996), "The surface temperature-vegetation index space for land cover and land-cover change analysis", *Int. J. Remote Sens.*, Vol. 17, pp. 463-87.

Lambin, E.F. and Ehrlich, D. (1997), "Land-cover changes in Sub-Saharan Africa (1982-1991): application of a change index based on remotely sensed surface temperature and vegetation indices at a continental scale", *Remote Sens. Environ.*, Vol. 61, pp. 181-200.

Lambin, E.F. and Strahler, A.H. (1994), "Change-vector analysis in multitemporal space: a tool to detect and categorize land-cover change processes using high temporal-resolution satellite data", *Remote Sens. Environ.*, Vol. 48, pp. 231-44.

Lieth, H. (1974), *Phenology and Seasonality Modeling*, Springer-Verlag, New York, NY.

Mainguet, M. (1994), *Desertification – Natural Background and Human Mismanagement*, 2nd ed., Vol. 1, Springer, Heidelberg,.

Nemani, R.R., Peirce, L., Running, S.W. and Goward, S. (1993), "Developing satellite derived estimates of surface moisture status", *J. Appl. Meteorology*, Vol. 32, pp. 548-57.

Otterman, J. (1974), "Baring high-albedo soils by overgrazing: a hypothesized desertification mechanism", *Science*, Vol. 186, pp. 531-3.

Otterman, J. (1996), "Desert-scrub as the cause of reduced reflectances in protected versus impacted sandy arid areas", *Int. J. Remote Sens.*, Vol. 17, pp. 615-9.

Price, J.C. (1984), "Land surface temperature measurements from the split window channels of the NOAA-7 advance very high resolution radiometer", *J. Geophysical Res.*, Vol. 89, pp. 7231-7.

Qin, Z. (2001), "A study of temperature change on both sides of the Israeli-Egyptian border: remote sensing and micrometeorological modeling", PhD thesis, Ben Gurion University of the Negev, Beer-Sheva.

Qin, Z. and Karnieli, A. (1999), "Progress in the remote sensing of land surface temperature and ground emissivity using NOAA-AVHRR data", *Int. J. Remote Sens.*, Vol. 20, pp. 2367-93.

Qin, Z., Dall'Olmo, G., Karnieli, A. and Berliner, P. (2001), "Derivation of split window algorithm and its sensitivity analysis for retrieving land surface temperature from NOAA-AVHRR data", *J. Geophysical Res.*, Vol. 106, pp. 22655-70.

Rao, C.R.N. and Chen, J. (1998), "Revised post-launch calibration of channels 1 and 2 of the advanced very high-resolution radiometer on board the NOAA-14 spacecraft", available at: http://psbsgi1.nesdis.noaa.gov:8080/EBB/ml/niccal1.html

Rouse, J.W., Haas, R.H., Schell, J.A., Deering, D.W. and Harlan, J.C. (1974), *Monitoring the Vernal Advancements and Retrogradation (Greenwave Effect) of Nature Vegetation*, NASA/GSFC Final Report, NASA, Greenbelt, MD.

Sellers, P.J. (1985), "Canopy reflectance, photosynthesis and transpiration", *Int. J. Remote Sens.*, Vol. 6, pp. 1335-72.

Tsoar, H. and Karnieli, A. (1996), "What determines the spectral reflectance of the Negev-Sinai sand dunes?", *Int. J. Remote Sens.*, Vol. 17, pp. 513-25.

Tucker, C.J. (1979), "Red and photographic infrared linear combination for monitoring vegetation", *Remote Sens. Environ.*, Vol. 8, pp. 127-50.

Tucker, C.J., Fung, I.Y., Keeling, C.D. and Gammon, R.H. (1986), "Relationship between atmospheric CO_2 variations and a satellite-derived vegetation index", *Nature*, Vol. 319, pp. 195-9.

UNEP (1992), *World Atlas of Desertification*, Edward Arnold Publishers, Sevenoaks.

Vermote, E., Tanré, D., Deuze, J.L., Herman, M. and Morcette, J.J. (1997), "Second simulation of the satellite signal in the solar spectrum (6S)", *IEEE Trans. Geosci. Remote Sens.*, Vol. 35, pp. 675-85.

Vogelmann, J.E. (1990), "Comparison between two vegetation indices for measuring different types of forest damage in north-eastern United States", *Int. J. Remote Sens.*, Vol. 11, pp. 2281-97.

Weinreb, M.P., Hamilton, G., Brown, S. and Koczor, R.J. (1990), "Nonlinearity corrections in calibration of advanced very-high resolution radiometer infrared channels", *J. Geophys. Res.*, Vol. 95 C5, pp. 7381-8.

Wilhite, D.A. and Glantz, M.H. (1985), "Understanding the drought phenomenon: the role of definitions", *Water International*, Vol. 10, pp. 111-20.